



## Effect of corrosive environment on fatigue property and crack propagation behavior of Al 2024 friction stir weld

Lei WANG, Li HUI, Song ZHOU, Liang XU, Bo HE

Department of Electromechanical Engineering, Shenyang Aerospace University, Shenyang 110136, China

Received 21 October 2015; accepted 3 March 2016

**Abstract:** In this investigation, 2024 aluminium alloy plates were friction stir welded, a sequence of experiments was performed including fatigue and crack propagation tests in air, under pre-corrosion and in a 3.5% NaCl solution, in combination with fractography analyses of near-threshold region, Paris region and final fracture region with the aid of scanning electron microscopy (SEM). Results showed that the corrosive environment caused a dramatical decrease in fatigue lives of FS welds, the corrosion fatigue lives of FS welds were almost a half of those of the as-welded specimens. The crack growth rates in FS welds were higher than their counterparts in base materials, under the corrosive environment, the crack growth rate differences between base materials and FS welds become increasingly apparent with the increase of stress intensity factor range  $\Delta K$ , but the pre-corrosion process had little effect on the FS welds' crack propagation behavior except for shortening the crack initiation lives greatly.

**Key words:** friction stir welding; aluminium alloy; fatigue; crack growth rate; corrosion

### 1 Introduction

High strength aluminium alloys are known to be attractive materials for aerospace industry because of their high specific strengths and low densities. The corrosion fatigue properties of high strength aluminium alloys have been widely studied over the past few years [1–6]. Nevertheless, according to the famous “wooden barrel effect” theory, the strength of a structure is determined by the weakest position, the weld of high strength aluminium alloy is considered to be the critical site and should be paid more attention, especially, when it is subjected to cyclic loads coupled with corrosive environment (termed corrosion fatigue), which plays a detrimental role in longevity of structures and in turn results in premature failure of components in service.

Friction stir welding (FSW) has recently been used to joint high strength aluminium alloys because of its solid-phase welding specialty comparing to traditional fusion welding, resulting in better weld quality and joint strength. The welding zone of aluminium alloy FS weld exhibits susceptibility to corrosion environment [7–9]. In previous work, it was determined that fatigue crack

propagation rate was slightly higher in FS weld than the base material counterpart for Al 7050, but it could reach up to two times higher in a 3.5% NaCl solution than that in air both in FS weld and heat affect zone because of the intergranular fracture mechanism in the corrosive environment for the sensitized grain boundaries caused by the FSW process [10]. The similar conclusion was given by UEMATSU et al [11], they found that the fatigue strength of FS weld in atmosphere was approximately the same as that of the parent material for Al 7075-T6, but the fatigue strengths of both the parent material and FS welds decreased to a greater extent in salt water than in atmosphere. CZECHOWSKI [12] found that the low-cycle fatigue life of the FS weld tested in the environments of 3.5% NaCl was much lower than the fatigue life obtained in air for 5083 and 5059 aluminium alloys, because the corrosion pits were connected with the increase in number potential positions of crack initiations and the presence of aggressive environment also affected crack growth by electrochemical dissolution or destruction caused by hydrogen.

Although many fatigue property investigations of aluminium alloy FS weld have been carried out in the

**Foundation item:** Project (51405309) supported by the National Natural Science Foundation of China; Project (L2014065) supported by the General Project of Scientific Research of Liaoning Provincial Education Department, China; Project (2013024011) supported by the Natural Science Foundation of Liaoning Province, China

**Corresponding author:** Lei WANG; Tel: +86-24-89728640; E-mail: [leiwang@sau.edu.cn](mailto:leiwang@sau.edu.cn)  
DOI: 10.1016/S1003-6326(16)64411-4

past decade [13–18], there are only few researches related to the corrosion fatigue behavior of aluminium alloy FS weld, especially for the effect of pre-corrosion defect on the fatigue behavior of FS weld.

This research studied the fatigue properties and fatigue crack growth rates of 2024-T4 aluminium alloy friction stir welds in air (with and without pre-corroded defects) and in a simulated seawater environment, the post-fracture surface morphology analyses were conducted to understand the mechanisms governing fracture under different test conditions.

## 2 Experimental

### 2.1 Material and specimen preparation

Starting material used in this study was 2024-T4 aluminium alloy in the form of 4 mm-thick plate, with the nominal chemical composition of 4.1% Cu, 0.4% Mn, 1.5% Mg, 0.3% Zn, 0.5% Fe, 0.5% Si, 0.15% Ti (mass fraction), and the corresponding mechanical properties are tabulated in Table 1.

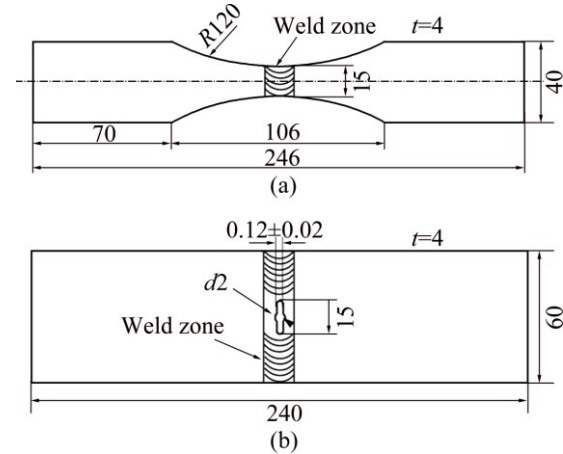
**Table 1** Mechanical properties of 2024-T4 alloy and 2024 FS weld

Material	Tensile strength/MPa	Yield strength/MPa	Elongation/%
2024-T4	467	350	15
2024 FS weld	411	298	6

FSW-3LM-4012 friction stir welding system was utilized to prepare the welded specimens parallel to the rolling direction with parameters of rotating speed 1000 r/min, welding velocity 100 mm/min and tilt angle 2°, then the flash and burr were cleaned up by an angle grinder. The dimensions of the welding tool were  $d15$  mm of the shoulder,  $d5$  mm and  $d4$  mm of the conical pin root and pin tip, respectively, and 3.7 mm of the pin length, with a right hand thread on the pin surface.

Fatigue and crack propagation specimens were cut from the welded plates as per ASTM E466-07 and ASTM E647-11 separately, as shown in Fig. 1. All the fatigue and crack propagation specimens were divided into three groups, one group was pre-corroded in a 3.5% NaCl solution (simulated seawater environment) for 48 h and then subjected to fatigue and crack propagation tests in air, another group was directly subjected to fatigue and crack propagation tests in a 3.5% NaCl solution environment, and the rest as-welded specimens were directly subjected to fatigue and crack propagation tests in air. The pre-corrosion process was conducted at room temperature (corrosive environment of  $(20 \pm 2)$  °C) with the pH value of the solution around 7, and then the corrosion products were removed using dilute nitric acid

and ultrasonic vibration cleaning equipment. Before the mechanical tests, all the specimens were scrubbed by cotton balls dipped in acetone solution and then put in the drying basin.



**Fig. 1** Schematic dimensions of fatigue specimen (a) and crack propagation specimen (b) (unit: mm)

### 2.2 Fatigue tests

The fatigue tests were performed in accord with ASTM E466 using an MTS 100 kN servo hydraulic machine under constant amplitude axial load with a stress ratio of  $R=0.06$ . The minimum stress was kept slightly above zero to prevent backlash in the grips at the minimum stress. The maximum stress was set at 140 MPa (sinusoidal loading) and the cycling rate was kept at the frequency of 10 Hz. For the corrosion fatigue tests, a sealed container full of 3.5% NaCl solution was utilized to keep the middle segment of the specimen containing the whole weld immersed in the corrosive environment.

### 2.3 Crack propagation tests

Crack propagation tests were performed in accord with ASTM E647 under stress ratio of 0.06 and frequency of 10 Hz using sinusoidal loading form, and a traveling optical microscope was utilized to monitor the crack propagation behavior continuously. Duplicate fatigue crack propagation tests were performed for each condition. As to the crack propagation tests in 3.5% NaCl solution, another sealed container was utilized to keep the middle segment of the MT specimen containing the weld immersed in the corrosive environment to ensure that the whole crack propagation process was inside the simulated seawater environment. The crack propagation tests of the base material (BM) were also carried out for comparison in all three conditions with the weld. The stress intensity factor range can be calculated according to Eq. (1) as follows:

$$\Delta K = \frac{\Delta P}{B} \sqrt{\frac{\pi \alpha}{2W}} \sec \frac{\pi \alpha}{2} \quad (1)$$

where  $\Delta K$  is the stress intensity factor range,  $\Delta P$  is the load range,  $B$  is the specimen thickness and  $\alpha=2a/W$  is the ratio of the crack length and the specimen width. The equation is effective within a certain range when  $2a/W \leq 0.9$ .

## 2.4 Fractography

The post-fracture surface morphologies were comprehensively examined in a Hitachi S-3400N scanning electron microscope (SEM) to determine the macro-fracture mode and characterize the micro-scale topography and mechanisms governing fracture under different situations.

## 3 Results and discussion

### 3.1 Results from fatigue tests

The fatigue test results of FS welds are listed and figured in Fig. 2. At the same stress level, the fatigue lives of friction stir welded specimens can reach around 160000, but the corrosive environment causes a dramatical decrease in fatigue lives of FS welds. After pre-corrosion, the fatigue lives of the welds decrease to around 100000, which are 64% those of the as-welded specimens, and the corrosion fatigue lives of FS welds are around 86000, which are almost a half of the as-welded specimens.

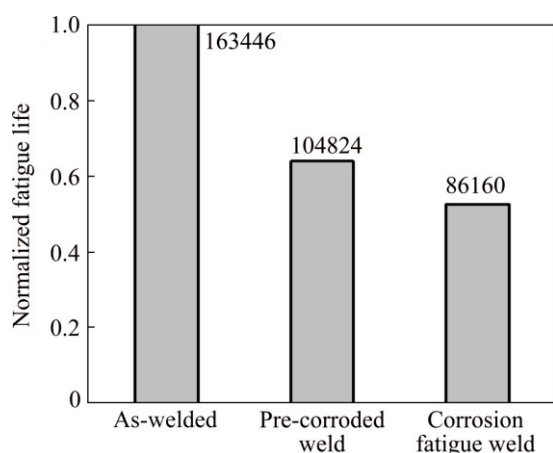


Fig. 2 Normalized fatigue lives of 2024 FS welds

As we know, aluminium alloy is sensitive to corrosive environment, which will cause pitting corrosion and result in a dramatical decrease in the crack initiation life, and finally shorten the whole fatigue life of the pre-corroded FS weld. Also, the corrosive environment will lead to grain boundary sensitization which could weaken the grain boundary binding force, as a result, the intergranular crack propagation will become easier and the crack growth rate will increase significantly. This can be verified by the post fracture analyses.

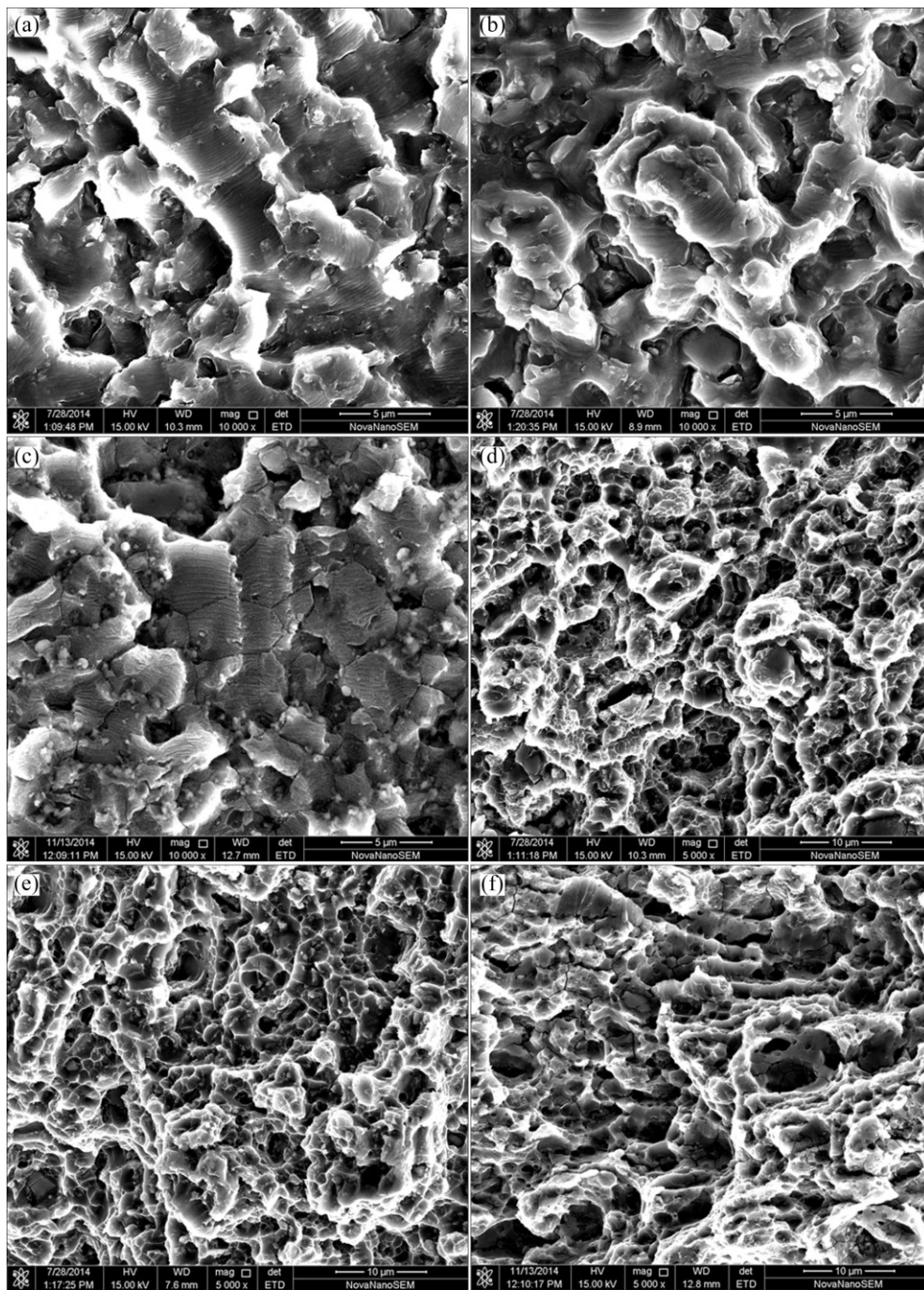
Representative fracture surface morphologies of 2024 FS welds from the fatigue tests are shown in Fig. 3, exhibiting mixed cracking mechanisms including striation and intergranular fracture features in all three type specimens. The fracture paths through the weld in air and with pre-corroded defects are quite similar in the fatigue crack growth region and final fracture region, while the fracture path through the weld in 3.5% NaCl solution shows some discriminative features both in the fatigue crack growth and final fracture region. In the fatigue crack growth region, the fracture surface of FS weld in 3.5% NaCl solution is more sensitive to intergranular cracking than those of FS welds in air and with pre-corroded defects, as shown in Figs. 3(a), (b) and (c), showing many intergranular secondary cracks and remaining corrosion products, and the striation space is larger than those of FS welds in air and with pre-corroded defects.

The final fracture surfaces of all three type specimens in Figs. 3(d), (e) and (f) submit to dimple rupture mechanism. Dimples are relatively uniform distributed in fractures of welds tested in air and with pre-corroded defects, while fracture of weld tested in 3.5% NaCl solution is composed of non-uniform dimples, with several secondary cracks between them. The result is mainly caused by the corrosive environment which leads to a reduction in plasticity of the weld and an easier intergranular cracking, and the high crack growth rate of the weld in 3.5% NaCl solution results in an increased strain rate of the material, this finally leads to the size variation of dimples.

### 3.2 Results from crack propagation tests

Fatigue crack growth rates in the base materials and FS welds in air, with pre-corroded defects and in 3.5% NaCl solution are shown, respectively, in Figs. 4, 5 and 6. Results show that all the crack growth rates in FS welds are higher than those of the base materials in three test conditions. At lower  $\Delta K$  near the threshold, the difference in fatigue crack growth rates between those in base materials and FS welds in air is insignificant with a comparable  $\Delta K_{th}$  approaching  $5 \text{ MPa} \cdot \text{m}^{-1/2}$ , while with the increase of the  $\Delta K$ , the fatigue crack growth rate difference becomes more obvious, as shown in Fig. 4. Note that there is an inflection point at the intermediate  $\Delta K$  around  $12 \text{ MPa} \cdot \text{m}^{-1/2}$  in the fatigue crack growth rate curve the friction stir weld, the reason should be the weak bonding or microdefects inside the weld which results in a sudden increase of the fatigue crack growth rate.

As shown in Fig. 5, the fatigue crack growth rate curves of base material and friction stir weld with pre-corroded defects are nearly parallel to each other with the friction stir weld curve on the top. Because of



**Fig. 3** Fracture surfaces of 2024 FS weld from fatigue specimens: (a, d) Fatigue crack growth areas and final fracture surfaces in air; (b, e) With pre-corroded defects; (c, f) In 3.5% NaCl solution

the protection of the  $\text{Al}_2\text{O}_3$  oxidation film for the base material, the pre-corrosion process caused less damage compared to the FS weld on which the oxidation film was destroyed during the welding process. As a result, the  $\Delta K_{th}$  of the friction stir weld decreased obviously, and the crack growth rate of the friction stir weld at lower  $\Delta K$  was enhanced compared with its counterpart in air.

In 3.5% NaCl solution, the crack growth rates of both base material and FS weld increase dramatically, as

shown in Fig. 6, especially with the increase of  $\Delta K$ , and the crack growth rate of FS weld improves faster than that of base material. Accordingly, both  $\Delta K_{th}$  of base material and FS weld decrease obviously lower than  $5 \text{ MPa} \cdot \text{m}^{-1/2}$ .

The effect of test conditions on the fatigue crack growth rates through base materials and FS welds can be better demonstrated in Fig. 7 by replotting the data shown in Figs. 4, 5 and 6. From Fig. 7, we can find that the fatigue crack growth rate of FS weld in 3.5% NaCl



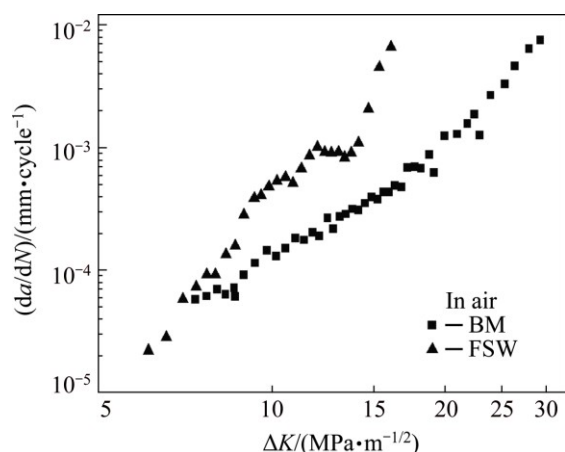


Fig. 4 Fatigue crack growth rates through 2024 base material and friction stir weld in air

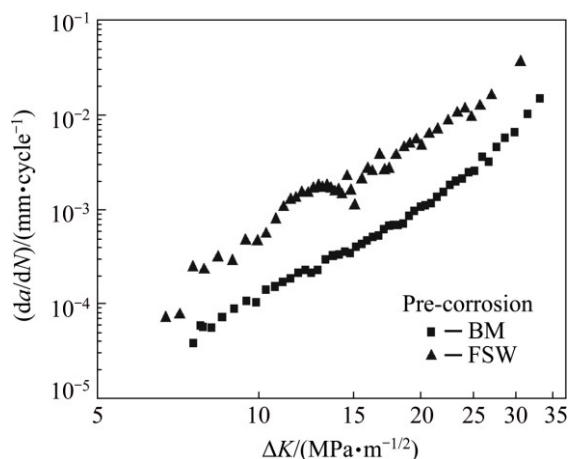


Fig. 5 Fatigue crack growth rates through 2024 base material and friction stir weld under pre-corrosion

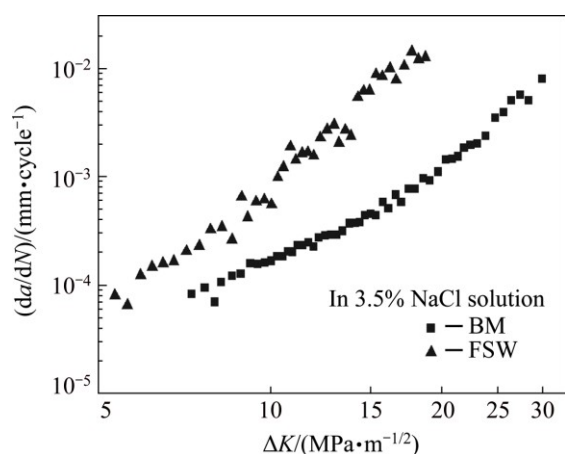


Fig. 6 Fatigue crack growth rates through 2024 base material and friction stir weld in 3.5% NaCl solution

solution has the highest value, indicating that the corrosive environment plays a detrimental role in the fatigue crack growth resistance of the FS weld. The pre-corrosion process just enhances the fatigue crack growth rate at lower  $\Delta K$ , but at high and intermediate  $\Delta K$ ,

the fatigue crack growth rates are similar to each other for FS welds with pre-corrosion defects and in air, except for the inflection caused by the possible defects inside the weld. At lower  $\Delta K$  near threshold, fatigue crack growth rates in base material and FS weld in air are comparable, while the FS welds with pre-corroded defects and in 3.5% NaCl solution have higher fatigue crack growth rates. With the increase of  $\Delta K$ , the difference in fatigue crack growth rates between base material and FS weld becomes significant, particularly in 3.5% NaCl solution.

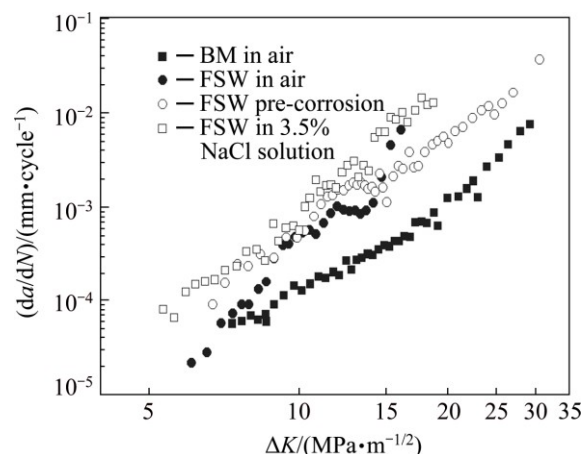


Fig. 7 Fatigue crack growth rates through 2024 under different conditions

The fatigue crack growth rates can be represented by Paris' law relation,  $da/dN = C(\Delta K)^m$ , where  $C$  is a dimensional constant and  $m$  is an exponent that represents the slope of the fatigue crack growth rate data in the log-log plot. The Paris' law equation can be obtained by fitting the fatigue crack growth rate data, Table 2 shows the fitting results of the experimental data from fatigue crack growth tests in base materials and FS welds in air, with pre-corroded defects and in the simulated seawater, respectively. All crack growth rates in FS welds are higher than their counterparts in base materials for each test condition. The crack growth rate differences between base material and FS weld become increasingly apparent with the increase of  $\Delta K$  for specimens in air and in 3.5% NaCl solution, but it is almost a constant value around 4.8 for the ratio of crack growth rates between base material and FS weld for specimens with pre-corroded defects, this is consistent with previous result from Fig. 5. When  $\Delta K$  is relative low at  $7 \text{ MPa}\cdot\text{m}^{-1/2}$ , the crack growth rates of FS welds are 1.6, 4.9 and 3.7 times respectively to those of base materials in three different conditions. Under the  $\Delta K$  value of  $10 \text{ MPa}\cdot\text{m}^{-1/2}$ , the crack growth rates of FS welds change to 3, 4.8 and 5.8 times respectively to their counterparts of base materials, while if the  $\Delta K$  increases to  $15 \text{ MPa}\cdot\text{m}^{-1/2}$ , the crack growth rates of FS welds are

**Table 2** Fitting results of fatigue crack growth data

Specimen	Fitting function	Crack growth rate/(10 <sup>-5</sup> mm·cycle <sup>-1</sup> )					
		$\Delta K=7$	$\Delta K=10$	$\Delta K=15$	$\Delta K=20$	$\Delta K=25$	$\Delta K=30$
BM in air	$\frac{da}{dN} = 5.138 \times 10^{-8} \times (\Delta K)^{3.354}$	3.51	11.6	45.2	119	251	–
BM pre-corrosion	$\frac{da}{dN} = 3.099 \times 10^{-8} \times (\Delta K)^{3.537}$	3.02	10.7	44.8	124	273	520
BM in seawater	$\frac{da}{dN} = 1.157 \times 10^{-7} \times (\Delta K)^{3.135}$	5.16	15.8	56.3	139	279	494
FSW in air	$\frac{da}{dN} = 3.265 \times 10^{-9} \times (\Delta K)^{5.026}$	5.77	34.7	266	–	–	–
FSW pre-corrosion	$\frac{da}{dN} = 1.569 \times 10^{-7} \times (\Delta K)^{3.519}$	14.8	51.8	216	594	1300	2480
FSW in seawater	$\frac{da}{dN} = 3.598 \times 10^{-8} \times (\Delta K)^{4.408}$	19.1	92.1	550	1950	–	–

Unit of  $\Delta K$  is MPa·m<sup>-1/2</sup>

5.9, 4.8 and 9.8 times to those of base materials, under a higher  $\Delta K$  of 20 MPa·m<sup>-1/2</sup>, it increases to 14 times for the crack growth rate ratio between FS weld and base material for specimens in 3.5% NaCl solution. As a result, we can get a conclusion that the pre-corrosion environment had a similar accelerating influence on crack growth rates of both base material and FS weld, which showed a constant difference ratio around 4.8, but the corrosion environment had a bigger accelerating influence on crack growth rates of FS welds, indicating that the FS weld is more sensitive to the corrosion environment compared with the base materials.

In Table 3, fracture surfaces of near-threshold region, Paris region and final fracture region from base materials and FS welds tested in three test conditions are tabulated for comparison. The fracture surfaces from crack propagation specimens of 2024 aluminium alloy have cleavage-like features in near-threshold region, showing river-like patterns in base materials. After friction stir welding, the fracture surfaces become rougher in near-threshold region. Some corrosion products and intergranular cracks exist at the fracture surfaces both in base materials and FS weld when the tests were performed in 3.5% NaCl solution.

In the Paris region, the crack propagation in the base material submitted mainly to the striation mechanism, accompanied by some slip features. As to the base material in 3.5% NaCl solution, the striation space was larger than those in air and with pre-corroded defects and some intergranular secondary cracks emerged on the fracture, representing a higher crack growth rate. The crack propagation in FS welds showed obvious mixed cracking features controlled by the striation mechanism and intergranular cracking mechanism, and the striations became discontinuous in different grains. Because of the acutely mechanical action during the friction stir welding process and followed dynamic recrystallization inside the FS weld,

the grains were crushed and recrystallized into fine equiaxed crystals, which are easier for intergranular cracking.

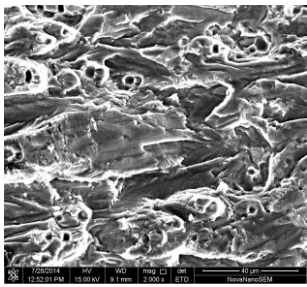
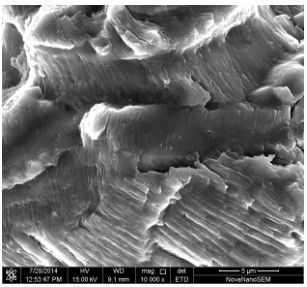
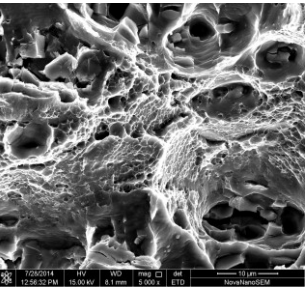
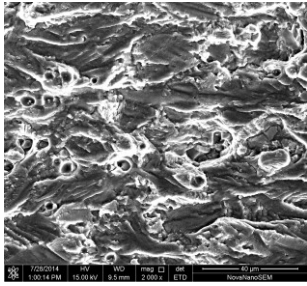
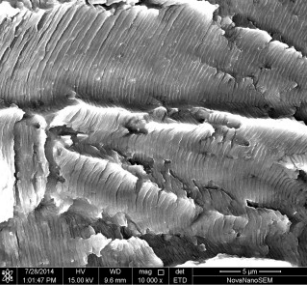
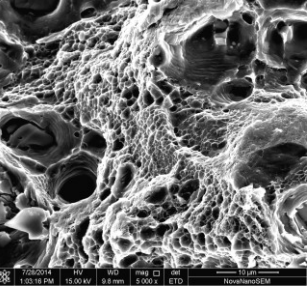
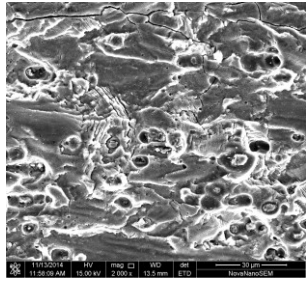
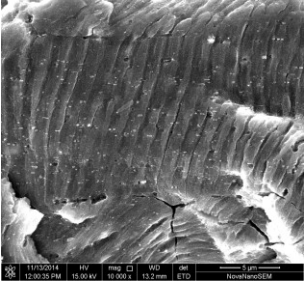
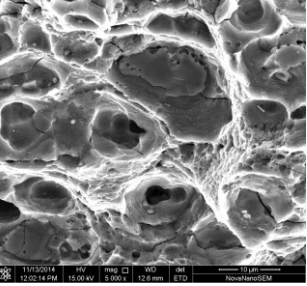
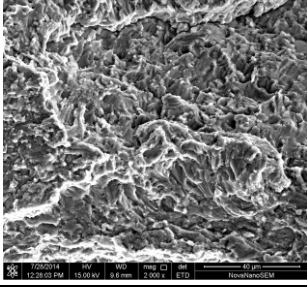
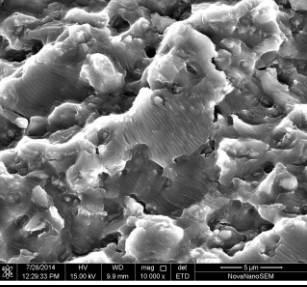
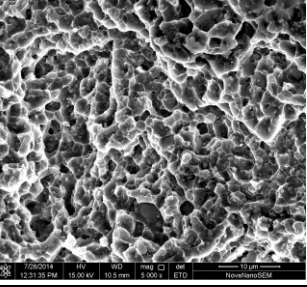
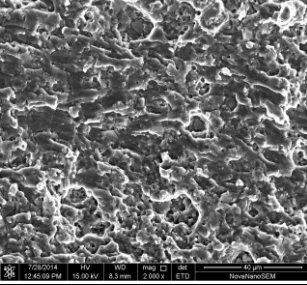
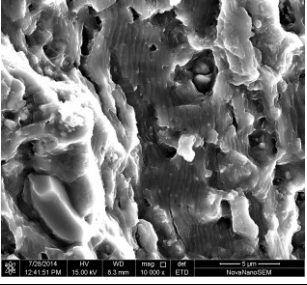
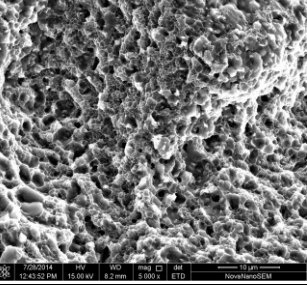
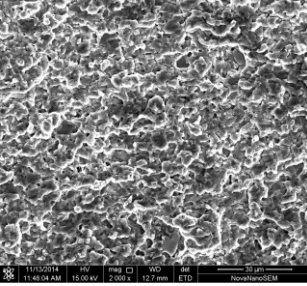

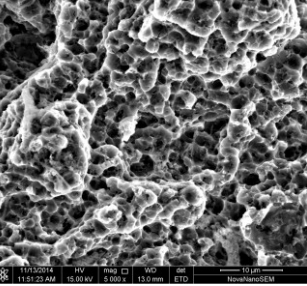
The final fractures of base materials and FS welds show obviously different features in the dimple sizes and distribution despite the test conditions. Dimples of the base material fractures are heterogeneously distributed with nonuniform dimple sizes, while the dimples of FS welds are homogeneously distributed with equiaxed fine dimple sizes. It is known that one of the main effects on the size of dimples are the dimension, shape and distribution of the secondary phase particles, because of the acutely forging and stirring action during the friction stir welding process, the heterogeneously distributed nonuniform secondary phase particles in the base material were crushed into small fragments and were uniformly distributed inside the weld, the nucleation of dimples will be affected by the secondary phase particles, as a result, the nonuniformly distributed dimples in the base material change into uniform fine ones inside the FS weld. Because of the decrease of the relative plasticity caused by the corrosion environment, dimples of the final fracture in the base material become shallow compared with the counterparts of base material in air and with pre-corroded defects.

## 4 Conclusions

1) In general, the corrosive environment caused a dramatical decrease in fatigue lives of FS welds, fatigue lives of FS welds with pre-corroded defects are about 64% of the as-welded specimens while the corrosion fatigue lives of FS welds in 3.5% NaCl solution are about a half those of the as-welded specimens.

2) Crack growth rates in FS welds are higher than those of the base materials in three test conditions. Fatigue crack growth rate of FS weld in 3.5% NaCl solution has the highest value, and the pre-corrosion

**Table 3** Fracture surfaces from crack propagation specimens

Material	Near-threshold region	Paris region	Final fracture
BM in air			
BM pre-corroded			
BM in seawater			
FSW in air			
FSW pre-corroded			
FSW in seawater			

process just enhances the fatigue crack growth rate at lower  $\Delta K$  near threshold. The crack growth rate differences between base material and FS weld become increasingly apparent with the increase of  $\Delta K$  for specimens in air and in 3.5% NaCl solution while it is almost a constant value for the ratio of crack growth rates between base material and FS weld for specimens under pre-corrosion.

3) In near-threshold region, the fracture surfaces have cleavage-like features showing river-like patterns. In the Paris region, the striation mechanism of base material changes into a mixed cracking mechanism including striation and some intergranular cracking features of FS welds. In 3.5% NaCl solution, the striation space is larger than those of FS welds in air and with pre-corroded defects. The nonuniformly distributed dimples in the base material change into uniform fine ones inside the FS weld in final fracture region.

## References

- [1] ROHLIN S I, KIM J Y, NAGY H, ZOOFAN B. Effect of pitting corrosion on fatigue crack initiation and fatigue life [J]. Engineering Fracture Mechanics, 1999, 62: 425–444.
- [2] CHLISTOVSKY R M, HEFFEMAN P J, DUQUESNAY D L. Corrosion-fatigue behaviour of 7075-T651 aluminum alloy subjected to periodic overloads [J]. International Journal of Fatigue, 2007, 29: 1941–1949.
- [3] CRAWFORD B R, LOADER C, LIU Q, HARRISON T J, SHARP P K. Can pitting corrosion change the location of fatigue failures in aircraft? [J]. International Journal of Fatigue, 2014, 61: 304–314.
- [4] HALL M M Jr. Effect of cyclic crack opening displacement rate on corrosion fatigue crack velocity and fracture mode transitions for Al–Zn–Mg–Cu alloys [J]. Corrosion Science, 2014, 81: 132–143.
- [5] CHEMIN A E A, SACONI F, FILHO W W B, SPINELLI D, RUCHERT C O F T. Effect of saline corrosion environment on fatigue crack growth of 7475-T7351 aluminum alloy under TWIST flight loading [J]. Engineering Fracture Mechanics, 2015, 141: 274–290.
- [6] GENEL K. Environmental effect on the fatigue performance of bare and oxide coated 7075-T6 alloy [J]. Engineering Failure Analysis, 2013, 32: 248–260.
- [7] PAGLIA C S, BUCHHEIT R G. A look in the corrosion of aluminum alloy friction stir welds [J]. Scripta Materialia, 2008, 58: 383–387.
- [8] WANG Qing-zhao, ZHAO Yong, YAN Keng, LU Sheng. Corrosion behavior of spray formed 7055 aluminum alloy joint welded by underwater friction stir welding [J]. Materials & Design, 2015, 68: 97–103.
- [9] SEETHARAMAN R, RAVISANKAR V, BALASUBRAMANIAN V. Corrosion performance of friction stir welded AA2024 aluminium alloy under salt fog conditions [J]. Transactions of Nonferrous Metals Society of China, 2015, 25: 1427–1438.
- [10] PAO P S, GILL S J, FENG C R, SANKARAN K K. Corrosion-fatigue crack growth in friction stir welded Al 7050 [J]. Scripta Materialia, 2001, 45: 605–612.
- [11] UEMATSU Y, TOKAJI K, TOZAKI Y, SHIBATA H. Fatigue behaviour of friction stir welded A7075-T6 aluminium alloy in air and 3% NaCl solution [J]. Welding International, 2013, 27: 441–449.
- [12] CZECHOWSKI M. Low-cycle fatigue of friction stir welded Al–Mg alloys [J]. Journal of Materials Processing Technology, 2005, 164: 1001–1006.
- [13] MA Y, XIA Z C, JIANG R R, LI W Y. Effect of welding parameters on mechanical and fatigue properties of friction stir welded 2198 T8 aluminum–lithium alloy joints [J]. Engineering Fracture Mechanics, 2013, 114: 1–11.
- [14] ILMAN M N, KUSMONO, ISWANTO P T. Fatigue crack growth rate behaviour of friction-stir aluminium alloy AA2024-T3 welds under transient thermal tensioning [J]. Materials & Design, 2013, 50: 235–243.
- [15] SIVARAJ P, KANAGARAJAN D, BALASUBRAMANIAN V. Fatigue crack growth behaviour of friction stir welded AA7075-T651 aluminium alloy joints [J]. Transactions of Nonferrous Metals Society of China, 2014, 24: 2459–2467.
- [16] BONI L, LANCIOTTI A, POLESE C. “Size effect” in the fatigue behavior of friction stir welded plates [J]. International Journal of Fatigue, 2015, 80: 238–245.
- [17] BESEL M, BESEL Y, MERCADO U A, KAKIUCHI T, UEMATSU Y. Fatigue behavior of friction stir welded Al–Mg–Sc alloy [J]. International Journal of Fatigue, 2015, 77: 1–11.
- [18] MA Yue, ZHAO Zhen-qing, LIU Bao-qi, LI Wen-ya. Mechanical properties and fatigue crack growth rates in friction stir welded nugget of 2198-T8 Al–Li alloy joints [J]. Materials Science and Engineering A, 2013, 569: 41–47.

# 腐蚀环境对 2024 铝合金搅拌 摩擦焊缝疲劳与裂纹扩展性能的影响

王磊, 回丽, 周松, 许良, 何波

沈阳航空航天大学 机电工程学院, 沈阳 110136

**摘 要:** 研究 2024 铝合金搅拌摩擦焊缝在空气、预腐蚀与 3.5% 盐水腐蚀液中的疲劳与裂纹扩展性能, 并采用 SEM 对断口的近门槛区、稳定扩展区与瞬断区进行观测。结果表明, 腐蚀环境对铝合金搅拌摩擦焊缝的寿命产生很大影响, 焊缝的腐蚀疲劳寿命只有空气中的一半左右; 焊缝的裂纹扩展速率比母材快, 在腐蚀环境下, 随着应力强度因子幅度的增大, 母材与焊缝裂纹扩展速率的差距越来越大, 但预腐蚀损伤对焊缝的裂纹扩展速率影响较小, 只是降低了裂纹萌生寿命。

**关键词:** 搅拌摩擦焊; 铝合金; 疲劳; 裂纹扩展; 腐蚀

(Edited by Yun-bin HE)